PNAS
www.pnas.org

Supplementary Information for

Feeding state sculpts a circuit for sensory valence in *Caenorhabditis elegans*

Sophie Rengarajan, Kristen A. Yankura, Manon L. Guillermin, Wendy Fung, and Elissa A. Hallem

Elissa Hallem
Email: ehallem@ucla.edu

This PDF file includes:

Supplementary text
Figs. S1 to S11
References for SI reference citations

www.pnas.org/cgi/doi/10.1073/pnas.1807454116

SI Materials and Methods

C. elegans strains

The following *C. elegans* strains are listed in the order in which they appear in the manuscript: N2 Bristol; CX11697 *kyIs536[flp-17::casp-3(p17)::SL2::GFP, elt-2::mCherry]; kyIs538[glb-5::casp-3(p12)::SL2::GFP, elt-2::mCherry]*; PS6028 *syEx1134[twk-3::CAM #1.1; pax-2::GFP]*; IK1405 *njEx568[ttx-3::YC3.60, ges-1::NLS-RFP]*; EAH240 *otIs181[dat-1::mCherry + ttx-3::mCherry]; akEx387[lin-15(+), dat-1::GFP, dat-1::ICE]*; RM2702 *dat-1(ok157)*; MT10661 *tdc-1(n3420)*; MT9455 *tbh-1(n3247)*; MT10661 *tdc-1(n3419)*; CX16355 *tdc-1(n3419); kyEx5578[gcy-13::tdc-1a::SL2::GFP]*; CX16257 *tdc-1(n3419); kyEx5550[tbh-1::tdc-1a::SL2::GFP]*; EAH339 *otIs181[dat-1::mCherry + ttx-3::mCherry]; akEx387[lin-15(+), dat-1::GFP, dat-1::ICE]; syEx1134[twk-3::YC3.60]*; EAH338 *otIs181[dat-1::mCherry + ttx-3::mCherry]; akEx387[lin-15(+), dat-1::GFP, dat-1::ICE]; njEx568[ttx-3::YC3.60, ges-1::NLS-RFP]*; EAH353 *tdc-1(n3419); syEx1134[twk-3::YC3.60]*; EAH354 *tdc-1(n3419); njEx568[ttx-3::YC3.60, ges-1::NLS-RFP]*; AX2073 *lin-15(n765ts); dbEx[flp-17::YC3.60, lin-15(+)]*; EAH268 *bruEx160[twk-3::casp-3(p17); twk-3::casp-3(p12); myo-2::dsRed]*; EAH284 *bruEx138[ttx-3::casp-3(p17); ttx-3::casp-3(p12); myo-2::dsRed]*; EAH319 *bruEx171[glr-3::casp-3(p17); glr-3::casp-3(p12); myo-2::dsRed]*; LX636 *dop-1(vs101)*; LX702 *dop-2(vs105)*; LX703 *dop-3(vs106)*; FG58 *dop-4(tm1392)*; CX13111 *dop-5(ok568)*; EAH337 *dop-6(ok2090)* 3x outcrossed; MT13952 *lgc-53(n4330)*; CX16632 *kyIs693[tdc-1::HisCl1::SL2::mCherry]*; DA1774 *ser-3(ad1774)*; FX02104 *ser-6(tm2104)*; CX13079 *octr-1(ok371)*; FX02146 *ser-6(tm2146)*; SSR660 *ser-6(tm2416); ser-6p::ser-6(gDNA)::GFP*; SSR769 *ser-6(tm2146); str-1p::ser-6(gDNA)::GFP*; VN441 *ser-6(tm2104); tzIs3[cre::GFP, lin-15(+)]; vnEx142[ceh-17::ser-6, lin-44::GFP]*; EAH334 *lin-15(n765ts); otIs181[dat-1::mCherry + ttx-3::mCherry]; akEx387[lin-15(+), dat-1::GFP, dat-1::ICE]; dbEx[flp-17::YC3.60, lin-15(+)]*; EAH352 *tdc-1(n3419); lin-15(n765ts); dbEx[flp-17::YC3.60, lin-15(+)];* RB1341 *nlp-1(ok1470);* and FX5158 *flp-16(tm5158)*.

C. elegans were reared on Nematode Growth Media (NGM) plates seeded with *E. coli* OP50 bacteria using standard conditions (1). Except for high-CO_2-cultivated worms, all worms were raised at ambient temperature (~22°C) and CO_2 (~0.038%). Some strains were occasionally raised at 15°C but moved to room temperature at least 12 h prior to experiments in order to prevent any effects of temperature shifts on behavior. CO_2-cultivated worms were raised as previously described (2). For these experiments, young adults were placed in a Tritech Research DigiTherm® incubator at 22°C and 2.5% CO_2; three days later, the next generation was tested in behavioral assays or calcium imaging experiments. EAH240 was generated by crossing OH7193 *otIs181[dat-1::mCherry + ttx-3::mCherry]; him-8(e1489)* (3) and VM6365 *lin-15(n765ts); akEx387[lin-15(+), dat-1::GFP, dat-1::ICE]* (4). No behavioral differences were observed between EAH240 and VM6365; EAH240 was therefore used for all behavioral experiments so that the loss of dopaminergic neurons could be confirmed by the loss of *dat-1::mCherry* expression. EAH337 was generated by outcrossing RB1680 *dop-6(ok2090)* three times to N2. EAH334, EAH339, and EAH338 were generated by crossing AX2073, PS6028, and IK1405 to EAH240, respectively. CX14373 *kyEx4571[tag-168::HisCl1::SL2::GFP, myo-3::mCherry]* was used as a control for Fig. S7 to confirm the efficacy of NGM plates containing 10 mM histamine.

CO_2-chemotaxis assays: Chemotaxis assays were performed as described (2, 5). Briefly, ~100-500 young adult worms were washed off seeded NGM plates into a 65 mm Syracuse watch glass. Worms were washed 3 times with 3 mL of M9 buffer and allowed to settle at the bottom of the dish. After supernatant removal, worms were transferred to a 1.5 cm x

1.5 cm piece of Whatman paper. The filter paper was flipped and worms were transferred onto the center of a 10 cm circular chemotaxis or NGM plate for testing. Gases (the test concentration of CO_2, either 10% or 21% O_2, and the balance N_2) were delivered through holes in the plate lid at a rate of 2 mL/min. All chemotaxis assays used 10% CO_2 unless otherwise indicated. Assays were run for 20 min. At the end of each assay, experiments were scored by counting the number of worms in the 2 cm circular scoring regions directly under the CO_2 and air sources (Fig. S1). A chemotaxis index (CI) was then calculated as:

$$CI = \frac{\#\ worms\ in\ CO_2\ region - \#\ worms\ in\ air\ control\ region}{\#\ worms\ in\ CO_2\ region + \#\ worms\ in\ air\ control\ region}$$

To check for directional bias from room vibration or other sources, assays were always run in pairs, with the CO_2 and air control gases oriented in opposite directions for the two plates. If the difference in CIs between these assays was ≥0.9, it was concluded that directional bias was strongly influencing behavior and the trials were excluded from analysis. Assay pairs were also discarded if, for at least one assay in the pair, fewer than 7 worms were counted in the combined scoring regions. Since AIY-ablated animals moved poorly in chemotaxis assays, if there was no directional bias within a pair of assays but only one of the assays had fewer than 7 worms move, the assay with at least 7 worms scored was included in the analysis. For transient silencing of neurons using the histamine-gated chloride channel HisCl1 (6), transgenic animals expressing HisCl1 were incubated on 10 cm NGM plates containing 10 mM histamine for 15 min prior to testing in a chemotaxis assay.

Starvation of animals prior to CO_2-chemotaxis assays: Worms were starved on 10 cm 2% NGM plates (1) lacking bacterial food. To prevent worms from crawling off of the plate during starvation, an annular-shaped ring of Whatman filter paper with an outer diameter of 7 cm and a width of 0.75 cm was dipped into a 20 mM copper chloride ($CuCl_2$) solution and transferred onto the 2% NGM plate. Copper is aversive to *C. elegans* and can be used to retain worms on the plate during starvation (7). Well-fed worms were washed off growing plates with M9 buffer (1) into a watch glass, washed 3 times in M9, and then transferred with Whatman paper to the center of the starvation plate within the $CuCl_2$-soaked ring. Worms were left on the plates during the period of starvation. Immediately prior to behavioral testing, the $CuCl_2$-soaked filter paper was removed and worms were washed off the plate and then washed 3 times with M9 before being transferred to an assay plate for testing.

Exogenous dopamine assays: A fresh stock solution of 1 M dopamine-HCl in ddH_2O was prepared each day. The stock solution was wrapped in aluminum foil and stored in a 4°C incubator to minimize oxidation of dopamine. To make dopamine-treated plates for worm incubation, 200 μL of the stock solution was added to each 10 cm 2% NGM plate to make a final concentration of 10 mM dopamine for the plate. For mock-treatment plates, 200 μL of ddH_2O was added to 2% NGM plates. The solutions were spread onto the plates, and the plates were closed and loosely covered with aluminum foil to dry. Within 15 min, worms were washed off food, washed 3 times as described above, and then added to the plates for the duration of food deprivation. For testing, 200 μL of the dopamine stock solution or ddH_2O was added to each chemotaxis plate as described above. Within 15 min, worms were washed off the incubation plates and transferred with a piece of 1.5 cm x 1.5 cm Whatman filter paper onto the testing plates. Assays were run as described above, except

that aluminum foil was loosely placed over the assay plates for the duration of the assay to limit light exposure. A 15% CO_2 stimulus was used for these experiments.

Calcium imaging: To select worms for calcium imaging, young adult worms were screened for expression of yellow cameleon YC3.60 in the neuron of interest. To starve worms for up to 6 h, YC3.60-expressing worms were picked off of seeded NGM plates onto unseeded NGM plates. Worms were allowed to crawl on the plate for 1 min to remove residual food. They were then picked to the center of a 2% NGM plate lined with a 20 mM $CuCl_2$-dipped annular Whatman paper, where they were left for the period of food deprivation. Calcium imaging was performed as described (2). Briefly, animals expressing YC3.60 in the neuron of interest (2, 8, 9) were placed on a 2% agarose pad made with 10 mM HEPES. Worms were glued onto the pad with Meridian Surgi-Lock glue. A chamber was fabricated from a 10 mm Petri dish with a hole on each side of the dish along the diameter. The chamber was secured onto the coverslip with beeswax. Two gas tanks were fitted with valves controlled by a ValveBank TTL pulse generator. Flow meters delivered gas to the chamber at a rate of 0.73-0.78 L/min. An air pulse was delivered for 20 s, followed by the test gas for 20 s, and then the air control for 40 s. In CO_2 trials, the test gas was either 15% CO_2 (for AIY recordings) or 10% CO_2 (for BAG and RIG recordings) in a background of 21% O_2, balance N_2. For air trials, the test gas was the same as the air control gas (21% O_2, balance N_2). Images were acquired in the YFP and CFP channels at 2 frames/s with an EM-CCD camera and AxioVision software. For analysis, regions of interest (ROIs) were selected for the soma (BAG, RIG) or process (AIY, zone 2 (10)) of the neuron of interest and a background region. The average intensity for YFP and CFP of the background ROI was subtracted from the average intensity for YFP and CFP of the neuron/process. YFP values were adjusted to correct for CFP signal bleed-through, and then the YFP to CFP ratio (YFP/CFP) was calculated. The data were linearly baseline-adjusted using the air periods before and after the gas stimulus as the baseline. Recordings were excluded from analysis if the YFP/CFP ratio during the baseline periods was not flat. For each experiment, the different genotypes or timepoints being investigated were tested in parallel.

To quantify responses, the response period was defined as the period beginning with the onset of the CO_2 stimulus and ending 10 s after the offset of the CO_2 stimulus. The maximum and minimum values of % $\Delta R/R_0$ were calculated during the response period. For AIY imaging, recordings were categorized as inhibitory or excitatory. To determine the threshold for these categories, data from the air control experiments were used. For each condition tested, the mean of the maximum and minimum values of % $\Delta R/R_0$ for the air control was calculated. Thresholds for responses were set as three standard deviations above the average maximum air response or 3 standard deviations below the average minimum air response. In cases where both maximum and minimum values exceeded the response thresholds due to an initial excitatory response followed by a delayed inhibitory response, recordings were counted as excitatory. Recordings where the most extreme value fell in between the thresholds for excitatory and inhibitory responses were considered non-responses and were excluded from analysis. Heatmaps were generated using Heatmap Builder (11). Heatmaps show % $\Delta R/R_0$ on a scale of -10 to +100 (BAG), -10 to +20 (RIG), or -10 to +10 (AIY); values outside this range are shown as saturating. The order of responses in the heatmaps was determined by hierarchical cluster analysis, using a paired group algorithm with Euclidean distance as a similarity measure.

Statistical Analysis: Statistical tests were performed using GraphPad Prism v6.07. All statistical tests used are noted in the figure legends. Heatmaps were generated using Heatmap Builder (11). Hierarchical cluster analysis was performed using PAST (12).

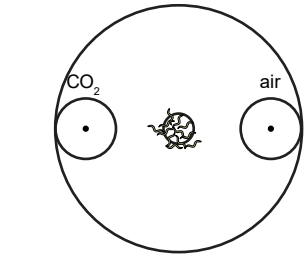

$$\text{chemotaxis index} = \frac{(\#\text{ at } CO_2 - \#\text{ at air})}{(\#\text{ at } CO_2 + \#\text{ at air})}$$

Figure S1. A CO_2 chemotaxis assay for *C. elegans*. Animals are placed in the center of a 10 cm plate, and a CO_2 gradient is established by delivering CO_2 into one side of the plate and an air control into the other. After the assay, the number of animals in the 2-cm-diameter circles under each gas inlet is counted and used to calculate the chemotaxis index according to the formula shown.

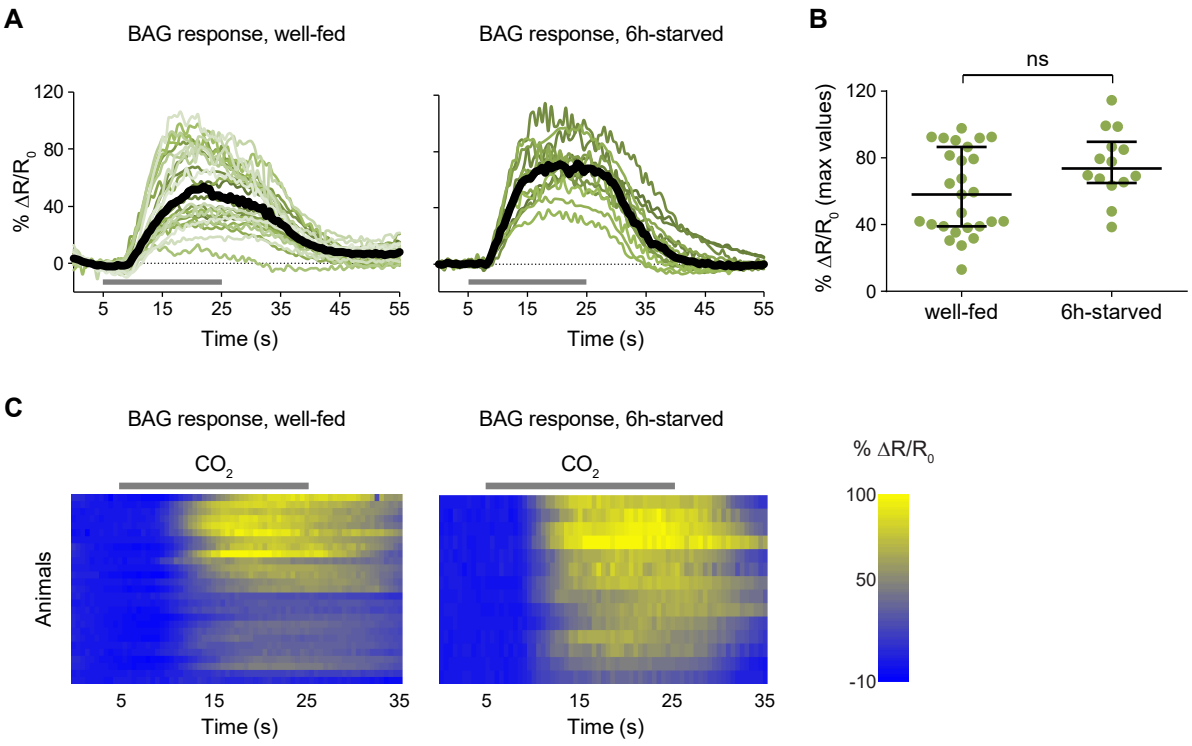

Figure S2. BAG neuron responses to CO_2 remain constant during starvation. BAG neurons respond similarly to CO_2 in well-fed and 6h-starved animals. n=14-27 animals per condition. ns=not significant (p=0.0581), Mann-Whitney test. In A, colored lines depict individual traces and black lines depict medians. In B, dots show maximum values of % $\Delta R/R_0$ for each animal; lines in dot plots show medians and interquartile ranges. In C, each row represents the response of an individual animal. Responses are ordered by hierarchical cluster analysis. In A and C, grey bars indicate the timing of the CO_2 pulse. Responses are to a 10% CO_2 stimulus.

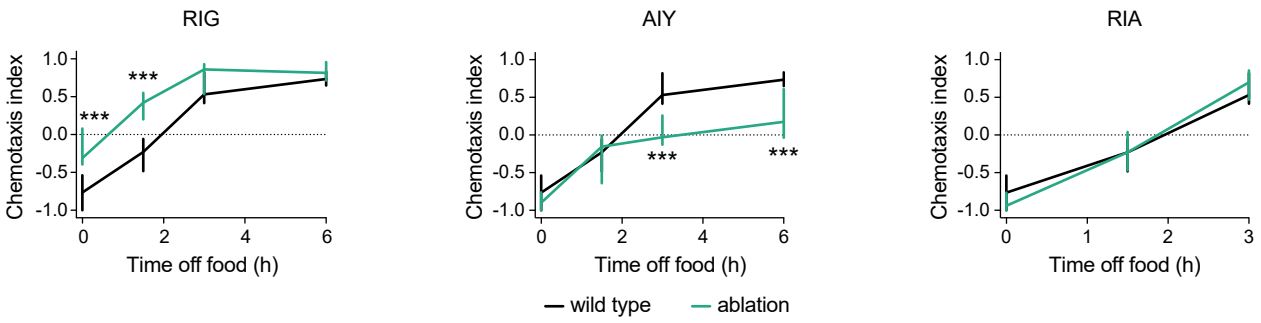

Figure S3. RIG and AIY interneurons, but not RIA interneurons, regulate CO_2 response during starvation. RIG-ablated animals show an accelerated shift to CO_2 attraction during starvation (left), while AIY-ablated animals fail to shift to CO_2 attraction (center). RIA-ablated animals show a normal shift to CO_2 attraction during starvation (right). n=6-18 trials per genotype and condition. ***p<0.001, two-way ANOVA with Sidak's post-test comparing wild-type and ablated animals at each time point. Lines show medians and interquartile ranges. Responses are to 10% CO_2.

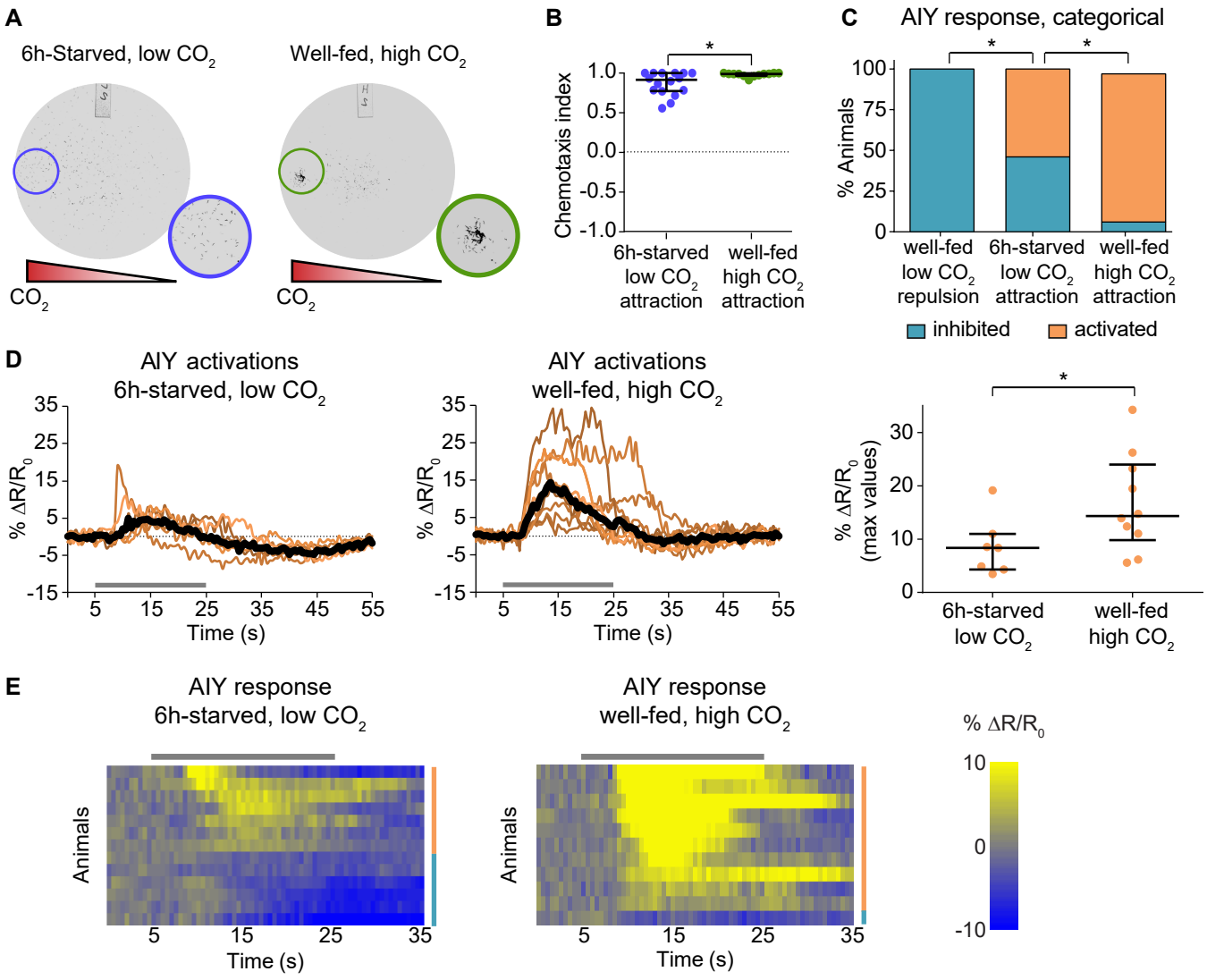

Figure S4. AIY activity correlates with behavioral sensitivity to CO_2. A-B. Animals cultivated in a high (2.5%) CO_2 environment display more robust CO_2 attraction than 6h-starved animals cultivated at ambient (0.038%) CO_2. n=12-16 trials per condition. *p<0.05, Kolmogorov-Smirnov test. Images show representative plates at the end of a chemotaxis assay. Lines in graph show medians and interquartile ranges. **C.** The categorical distribution of CO_2-evoked responses in AIY is altered by feeding state and cultivation condition. n=10-13 animals per condition. *p<0.05, chi-square test with Bonferroni post-test. **D-E.** Well-fed animals cultivated at high CO_2 show larger CO_2-evoked excitatory responses than 6h-starved animals cultivated at ambient CO_2. *p<0.05, Mann-Whitney test. Dot plot shows maximum values of % $\Delta R/R_0$ for the excitatory responses of each animal; lines in dot plots show medians and interquartile ranges. In D (left and center), colored lines depict individual traces and black lines depict medians. In E, each row represents the response of an individual animal. Responses are ordered by hierarchical cluster analysis; orange and blue coding indicates excitatory and inhibitory responses, respectively. In D-E, grey bars indicate the timing of the CO_2 pulse. Only excitatory responses are shown in D, whereas both excitatory and inhibitory responses are shown in E. A-B show responses to 10% CO_2; C-E show responses to 15% CO_2.

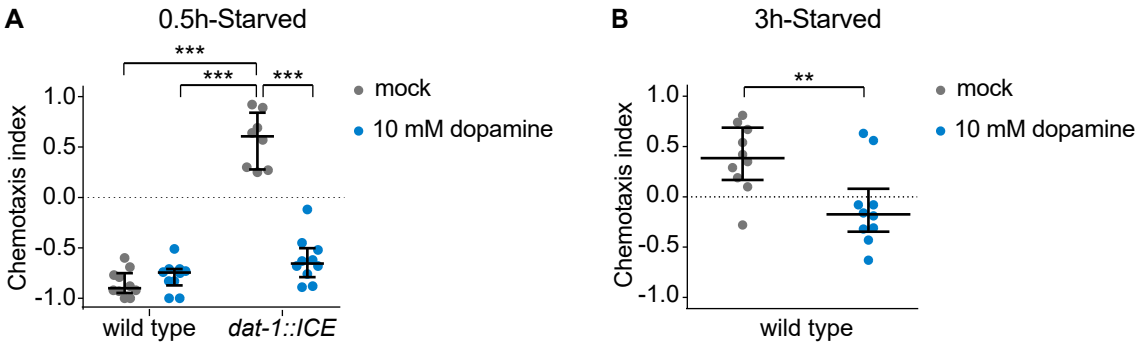

Figure S5. Exogenous dopamine treatment modulates responses to CO_2. A. Exogenous dopamine treatment (blue) restores CO_2 avoidance in *dat-1::ICE* animals food-deprived for 0.5 h. n=8-10 trials per condition. ***p<0.001, two-way ANOVA with Sidak's post-test. **B.** Exogenous dopamine treatment during starvation attenuates CO_2 attraction. n=10 trials per condition. **p<0.01, unpaired t-test with Welch's correction. Responses are to 15% CO_2.

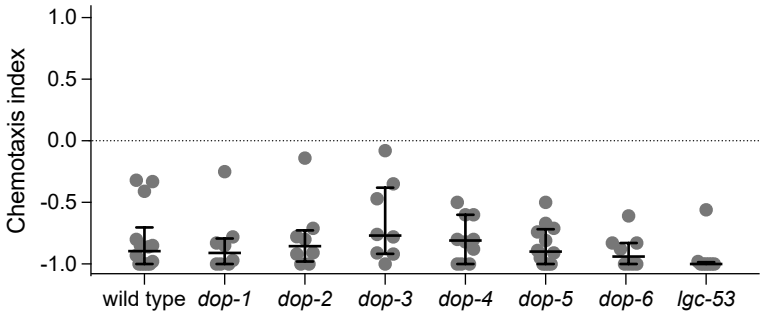

Figure S6. No single dopamine receptor is required for CO_2 avoidance in well-fed animals. Well-fed animals lacking individual dopamine receptors show normal CO_2 avoidance. n=8-14 trials per genotype. No significant differences were detected among genotypes (p=0.2479, Kruskal-Wallis test). Responses are to 10% CO_2. Lines show medians and interquartile ranges.

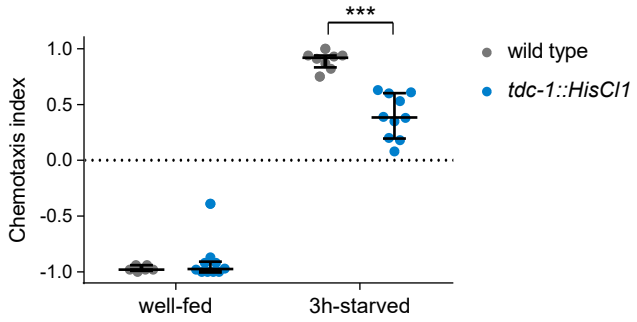

Figure S7. Transient silencing of *tdc-1*-expressing neurons (*tdc-1::HisCl1*) decreases CO_2 attraction in 3h-starved animals. n=6-10 trials per genotype and condition. ****p*<0.001, two-way ANOVA with Sidak's post-test. Lines show medians and interquartile ranges. Responses are to 10% CO_2.

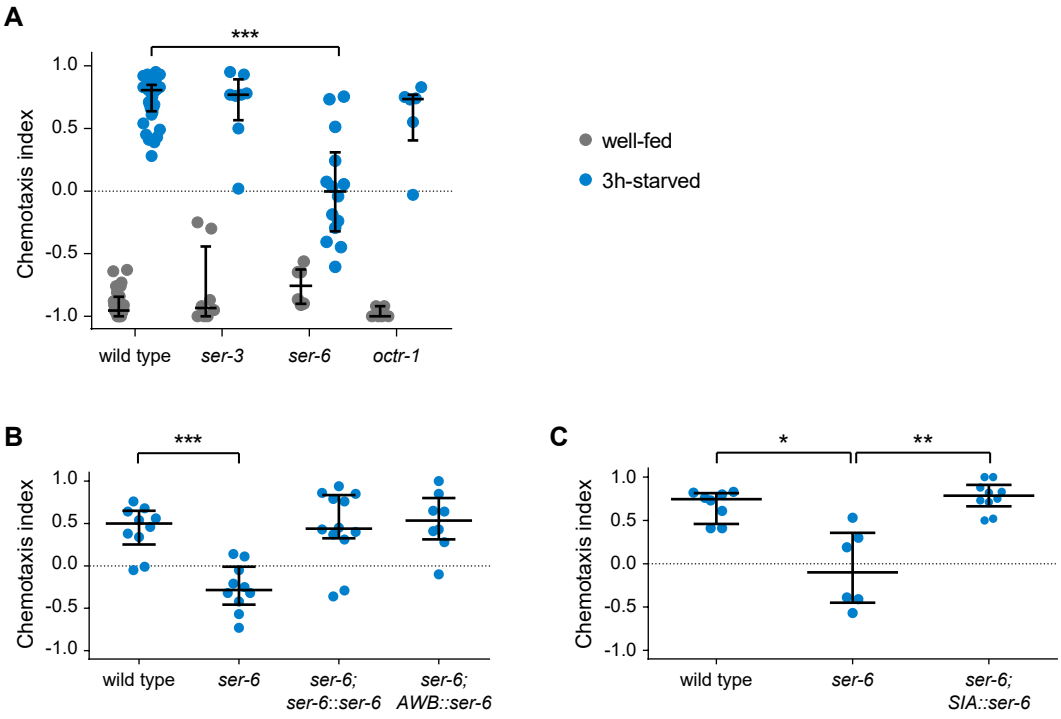

Figure S8. The octopamine receptor SER-6 is required for CO_2 attraction in starved animals. A. Animals lacking the octopamine receptor gene *ser-6* show normal CO_2 avoidance when well-fed but do not show CO_2 attraction when starved for 3 h. In contrast, animals lacking the octopamine receptor genes *ser-3* and *octr-1* respond normally to CO_2. n=6-36 trials per genotype and condition. ***p<0.001, two-way ANOVA with Dunnett's post-test. The *ser-6* allele tested was *ser-6(tm2104)*. **B.** Restoring *ser-6* function to *ser-6* mutants in either all of the *ser-6*-expressing neurons (*ser-6; ser-6::ser-6*) or AWB neurons (*ser-6; AWB::ser-6*) rescues CO_2 attraction in 3h-starved animals. n=8-12 trials per genotype. ***p<0.001, one-way ANOVA with Dunnett's post-test comparing each genotype to the wild-type control. The *ser-6(tm2416)* allele was used for this experiment. **C.** Restoring *ser-6* function to *ser-6* mutants in the SIA neurons (*ser-6; SIA::ser-6*) also restores CO_2 attraction in 3h-starved animals. n=6-10 trials per genotype. *p<0.05; **p<0.01, Kruskal-Wallis test with Dunn's post-test. The *ser-6(tm2104)* allele was used for this experiment. Responses are to 10% CO_2. Lines show medians and interquartile ranges.

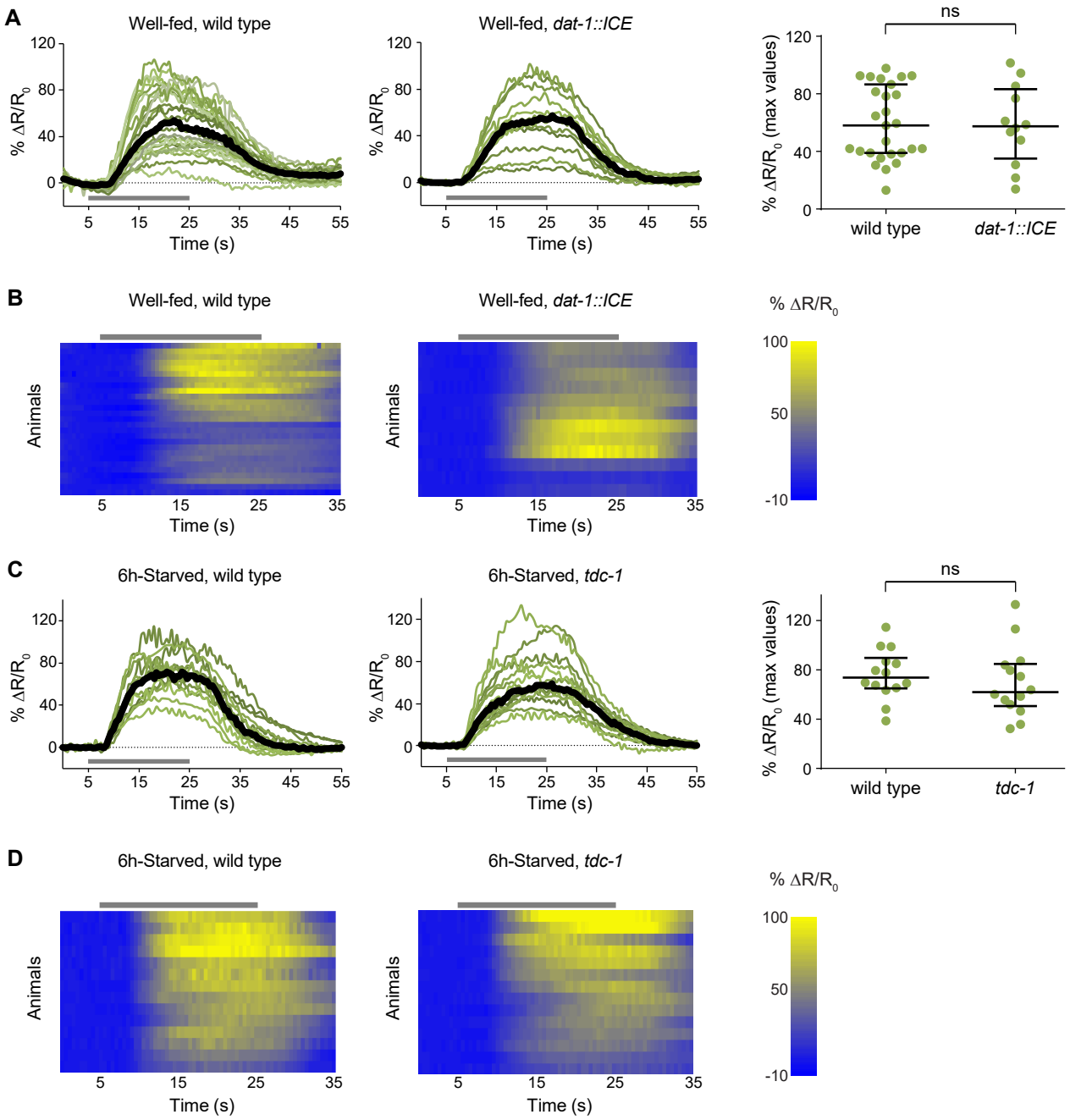

Figure S9. Loss of dopaminergic or octopaminergic signaling does not affect the CO_2-evoked activity of the BAG sensory neurons. A-B. The BAG neurons of well-fed wild-type and *dat-1::ICE* animals respond similarly to CO_2. n=12-27 animals per genotype. ns=not significant (p=0.9821), Mann-Whitney test. **C-D.** The BAG neurons of 6h-starved wild-type and *tdc-1* animals respond similarly to CO_2. n=14 animals per genotype. ns=not significant (p=0.5086), unpaired t-test with Welch's correction. In A and C, colored lines depict individual traces and black lines depict medians. In B and D, each row represents the response of an individual animal. Responses are ordered by hierarchical cluster analysis. In A-D, grey bars indicate the timing of the CO_2 pulse. Dot plots show maximum values of % $\Delta R/R_0$ for each animal; lines show medians and interquartile ranges. Data for wild-type animals is also shown in Fig. S2. Responses are to a 10% CO_2 stimulus.

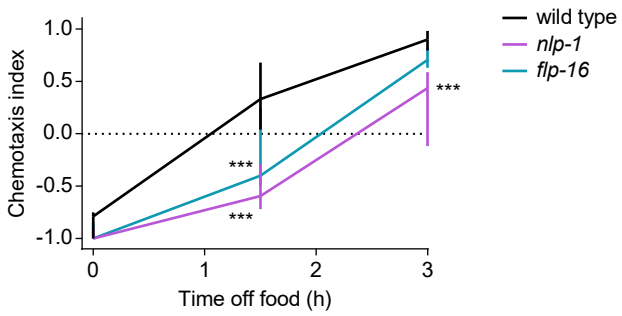

Figure S10. Neuropeptide signaling regulates CO_2 response during starvation. Relative to wild-type animals, *nlp-1* and *flp-16* animals show a delayed shift to CO_2 attraction during starvation. n=12-14 trials per genotype and condition. ***p<0.001, two-way ANOVA with Sidak's post-test. Responses are to 10% CO_2. Lines show medians and interquartile ranges.

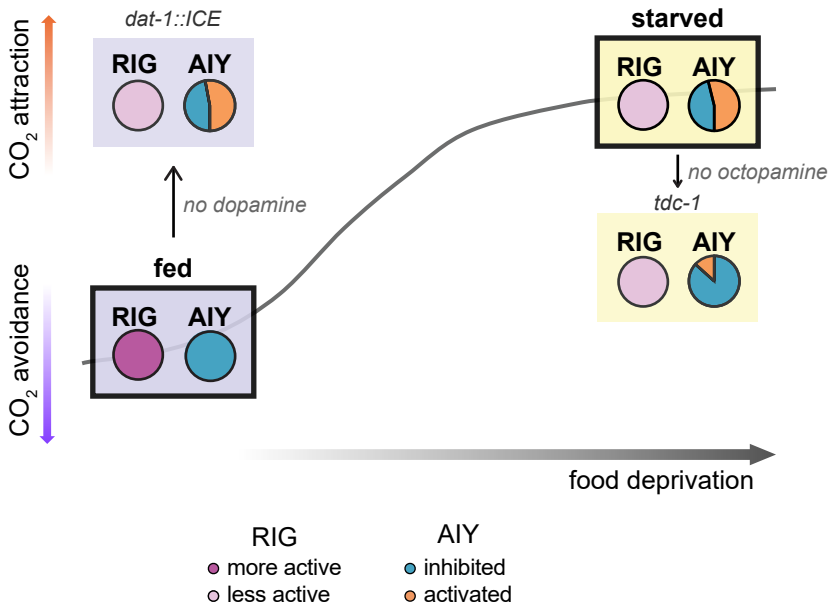

Figure S11. A model of how feeding state regulates CO_2 response valence. The gray curve in the background is a schematic depiction of CO_2 response following food deprivation. Boxes along the curve show schematic depictions of RIG and AIY activity in fed and starved animals. Dopamine promotes CO_2 avoidance in well-fed animals, and well-fed animals lacking dopamine (*dat-1::ICE*) adopt a circuit state resembling that of starved animals. Conversely, octopamine promotes CO_2 attraction in starved animals, and starved animals lacking octopamine (*tdc-1*) adopt a circuit state in which AIY neuron activity more closely resembles that of well-fed animals. Dark purple = excitatory activity in RIG; light purple = reduced excitatory activity in RIG; blue = inhibitory activity in AIY; orange = excitatory activity in AIY.

SI References

1. Stiernagle T (2006) Maintenance of *C. elegans*. In WormBook, www.wormbook.org, 1-11. Accessed December 1st, 2018.
2. Guillermin ML, Carrillo MA, & Hallem EA (2017) A single set of interneurons drives opposite behaviors in *C. elegans*. *Curr Biol* 27:2630-2639.
3. Flames N & Hobert O (2009) Gene regulatory logic of dopamine neuron differentiation. *Nature* 458:885-889.
4. Hills T, Brockie PJ, & Maricq AV (2004) Dopamine and glutamate control area-restricted search behavior in *Caenorhabditis elegans*. *J Neurosci* 24:1217-1225.
5. Carrillo MA, Guillermin ML, Rengarajan S, Okubo R, & Hallem EA (2013) O_2-sensing neurons control CO_2 response in *C. elegans*. *J Neurosci* 33:9675-9683.
6. Pokala N, Liu Q, Gordus A, & Bargmann CI (2014) Inducible and titratable silencing of *Caenorhabditis elegans* neurons *in vivo* with histamine-gated chloride channels. *Proc Natl Acad Sci USA* 111:2770-2775.
7. Campbell JC, Chin-Sang ID, & Bendena WG (2017) A *Caenorhabditis elegans* nutritional-status based copper aversion assay. *J Vis Exp* 125:e55939.
8. Kuhara A & Mori I (2006) Molecular physiology of the neural circuit for calcineurin-dependent associative learning in *Caenorhabditis elegans*. *J Neurosci* 26:9355-9364.
9. Bretscher AJ*, et al.* (2011) Temperature, oxygen, and salt-sensing neurons in *C. elegans* are carbon dioxide sensors that control avoidance behavior. *Neuron* 69:1099-1113.
10. Colon-Ramos DA, Margeta MA, & Shen K (2007) Glia promote local synaptogenesis through UNC-6 (netrin) signaling in *C. elegans*. *Science* 318:103-106.
11. King JY*, et al.* (2005) Pathway analysis of coronary atherosclerosis. *Physiol Genomics* 23:103-118.
12. Hammer Ø, Harper DAT, & Ryan PD (2001) PAST: Paleontological statistics software package for education and data analysis. *Palaeontol Electronica* 4:1-9.